

Original Article

Radix Rehmannia Glutinosa inhibits the development of renal fibrosis by regulating miR-122-5p/PKM axis

Xinhua Liu¹, Honglan Xu⁴, Yunhua Zang², Weiguo Liu³, Xiangbo Sun¹

Departments of ¹Nephrology, ²Neurology, ³Orthopedics and Traumatology, Hiser Medical Center of Qingdao, Qingdao 266000, Shandong Province, China; ⁴Department of Nephrology, Qingdao Municipal Hospital, Qingdao 266011, Shandong Province, China

Received August 12, 2021; Accepted October 20, 2021; Epub January 15, 2022; Published January 30, 2022

Abstract: Objective: It is acknowledged that Radix Rehmanniae Praeparata (RR) can regulate hormone metabolism, reduce blood glucose, resist aging, help to sedate patients and promote diuresis. The study aims to investigate the mechanism of how RR influences the development of renal fibrosis by regulating the miR-122-5p/PKM axis. Methods: Unilateral ureteral obstruction (UUO) was applied to induce renal fibrosis in mice *in vivo*, and human tubular epithelial HK2 cells treated by transforming growth factor- β (TGF- β 1) were used to induce renal fibrosis *in vitro*. Interleukin 6 (IL-6) and tumor necrosis factor- α (TNF- α) in mouse serum were detected by Enzyme-linked immunosorbent assay (ELISA); fibronectin (FN) and type I collagen (Col-I) in renal tissue were detected by Western blotting; serum creatinine (Cr) and blood urea nitrogen (BUN) were analyzed by kits. Hematoxylin-eosin (HE) staining and Masson staining were utilized to assess the degree of pathological damage and fibrosis. Cell viability and apoptosis in the *in vitro* model were detected by MTT and Flow cytometry. Dual-luciferase reporter assay was performed to determine intermolecular targeting relationships. Results: RR could inhibit IL-6 and TNF- α levels, decrease the levels of FN and Col-I and improve the renal function indexes (serum Cr and BUN) in UUO mice (all $P < 0.05$). In addition, RR was able to promote the up-regulation of miR-122-5p expression in UUO mice *in vivo* ($P < 0.05$). MiR-122-5p expression was down-regulated and PKM expression was up-regulated in HK2 cells treated with TGF- β 1 (all $P < 0.05$). RR inhibited renal fibrosis progression by regulating the miR-122-5p/PKM axis. Inhibition of miR-122-5p or overexpression of PKM could promote apoptosis of TGF- β 1-treated HK2 cells, inhibit their viability, aggravate fibrosis, and attenuate the protective effect of RR on the cells. The protective effect of RR promoted by overexpression of miR-122-5p was partially counteracted by PKM. Conclusion: RR can inhibit renal fibrosis progression by regulating the miR-122-5p/PKM axis.

Keywords: Radix Rehmannia Glutinosa, renal fibrosis, miR-122-5p, PKM

Introduction

Renal fibrosis is prevalent in end-stage renal diseases and it is a major cause of renal failure [1, 2]. Renal fibrosis is mainly characterized by tubular atrophy and extracellular matrix accumulation [3]. At present, the incidence of primary or concurrent renal diseases continues to increase [4]. This study strives to explore new molecular pathways and potential targets for the prevention and treatment of renal fibrosis. Radix Rehmanniae Praeparata (RR) is made from Radix Rehmanniae after steaming and further-processing, which belongs to the Scrophulariaceae family. It has been used as a medicine for more than 3000 years [5, 6].

Studies have demonstrated that RR has pharmaceutical effects such as anti-osteoporosis, anti-diabetes, anti-cardiovascular disease and anti-oxidative stress [7-10]. It has also been found that RR and *Cornus officinalis* can reduce symptoms of diabetic nephropathy via AGE-RAGE signaling pathway [11]. In this study, we further investigated the molecular mechanism of RR.

MiRNAs are a kind of single-stranded non-coding small RNAs that play a regulatory role during gene expression after transcription [12]. Many studies have suggested that miRNAs are involved in the pathogenesis of renal fibrosis. For example, miRNA let-7i-5p aggravates renal

The effect of RR in renal fibrosis

fibrosis by targeting GALNT1 [13]. Inhibition of CTCF-regulated miR-185-5p attenuates renal interstitial fibrosis in chronic renal diseases [14]. CircRNA30032 promotes renal fibrosis in mice with unilateral ureteral obstruction (UUO) through regulating miR-96-5p/HBEGF/KRAS axis [15]. Aristolochic acid has been reported to cause renal injury and tubulointerstitial fibrosis, and the expression level of the anti-fibrotic factor miR-122-5p was significantly reduced in mice of the aristolochic acid treatment group, but the function of miR-122-5p was not further elaborated [16]. In this study, we found that miR-122-5p had a binding site with PKM via search of a bioinformatics website and our experiments, and there is a targeted regulatory relationship between them. PKM is a pyruvate kinase that can be divided into two types, M1 and M2, and it has been reported that overexpression of PKM2 activates fibroblasts and induces renal interstitial fibrosis [17].

Based on the above studies, the specific roles of RR, miR-122-5p and PKM in nephropathy have all been clearly elaborated. The innovation of this study is elaborating the biological role of RR and investigating whether RR acts through miR-122-5p and PKM, which has not been mentioned in previous studies. An UUO model and an *in vitro* injury model induced by TGF- β 1 were established. We started with the exploration of RR effect on renal fibrosis and then investigated the specific molecular mechanisms affecting the development of this disease, so as to provide new ideas for its prevention and treatment.

Materials and methods

Bioinformatics analysis

We searched microarrays containing data related to renal fibrosis in the Gene Expression Omnibus database (GeneExpressionOmnibus, GEO); the Limma package was applied to analyze differential gene analysis of expression profiles, and the pheatmap package was included to draw heat maps. StarBase (<http://starbase.sysu.edu.cn/index.php>) and TargetScan (http://www.targetscan.org/vert_71/) were adopted for analyzing downstream target genes of miRNAs, DAVID online (<https://david.ncifcrf.gov/>) for PATHWAY enrichment analysis of target genes, DisGENET (<http://disgenet.org/search>) for retrieving risk genes associated

with renal fibrosis incidence, STITCH (<http://stitch.embl.de>) for analyzing RR-related genes and STRING (<http://string-db.org/>) for protein interaction analysis.

RR preparation

RR was purchased from Affiliated Hospital of Shandong University of Traditional Chinese Medicine. The quality of RR was guaranteed by HPLC-ELSD, and glucose and fructose were used as standards for quality identification (ZorbaxRX-SIL column was 4.6×200 mm; flow rate was 1 mL/min; mobile phase consisted of acetonitrile and water at 95:5). Drift tube temperature was set at 105°C; column temperature was 25°C; carrier gas flow rate was 2.5 mL/min; and fructose and glucose contents were above 7.5% and 6.5%, respectively.

Animal modeling and grouping

The unilateral ureteral obstruction (UUO) model was established based on the previous study [18]. The animal experiments in this study were in accordance with the guidelines of local institutional animal care and use committee. A total of 332 male C5BL/6J7 mice of SPF grade, at the age of 22 months, with the weight of 22±2 g, were provided by Vital River Laboratory Animal Technology Co., Ltd. (Beijing, China). They were adaptively fed at room temperature (about 20°C) for 1 week and exposed to light/dark for 12 h/12 h as a cycle. The mice were randomly divided into three groups, namely Sham group (n=10), UUO group (n=11), and UUO + RR group (n=11). Mice were anesthetized with intraperitoneal injection of 35 mg/kg pentobarbital sodium (Shanghai Zhongxi Pharmaceutical Co., Ltd., China). The abdominal skin was disinfected and incised. After the abdominal cavity was exposed, the left ureter was separated for ligation. Then ligation was performed 15 mm below the renal pelvis, and the abdominal cavity was sutured. The abdominal cavity of mice in the Sham group was immediately sutured without any treatment after dissection of the left ureter. Mice in the UUO + RR group were given intragastric administration of RR (0.2 mL/10 g body weight), and mice in the control group were given the same dose of phosphate buffered saline (PBS). Medication was given for 7 days, which was started on the first day of modeling. After anesthesia with intraperitoneal injection of 40 mg/

The effect of RR in renal fibrosis

Table 1. Sequence of cell transfection plasmid

inh-miR-122-5p	AAATCGAGCGACGTATTCAGCGAT
miR-122-5p mimic	GGCTATCATCAGCGAGCGACT
pcDNA-PKM	TTCGTTGACCAAGCATCTTCATTGCGCCGC
inhibitor NC	GGCATTCAAGCGAGCGC
mimic NC	ATCTAGCCGGCGCTCATCTAT
pcDNA	TACGAAGCGACTCTCGGAATC

kg pentobarbital sodium, the mice were sacrificed by cervical dislocation. Blood samples were collected and centrifuged at 4°C for 20 minutes at a rate of 1000× g. 0.5 mL serum and left renal tissues were collected from each mouse for analysis. We finally had one mouse eliminated from the UUO group and UUO + RR group respectively with 91% success rate of modeling. This study was performed in compliance with the standard of laboratory animal management and approved by the ethics committee of our hospital.

Renal function assessment

Serum creatinine (Cr) and blood urea nitrogen (BUN) were measured to assess renal function. Blood samples were collected, centrifuged at 2000× g for 15 min under 4°C. The supernatant samples were collected and tested according to the instructions of the Creatinine (Serum) Assay Kit (700460-2, AmyJet Scientific Incorporation, Wuhan, China). As for the BUN detection, the tissues were homogenized with 5 ml distilled water on ice, centrifuged at 13,000× g for 15 min under 4°C. The supernatant samples were also taken. The level of BUN was detected using the commercial kit (BC1535, Solaibao Life Science Co., Ltd., Beijing, China) and was read at the wavelength of 630 nm.

Assessment of renal pathological damage

Renal tissues were fixed using 4% paraformaldehyde. After 24 h, tissues were dehydrated and routinely embedded in paraffin, and then stained with hematoxylin-eosin (HE) staining (G1120, Solaibao Life Science Co., Ltd., Beijing, China). Tissues were stained in hematoxylin solution for 10 min and eosin solution for 1 min, dehydrated to be transparent, sealed with neutral gum, observed under a microscope and evaluated with scores according to the fibrosis degree, with 0 for no fibrosis, 1 for 10% fibrosis, 2 for 11-25% fibrosis, 3 for 26-45% fibrosis, 4

for 46-75% fibrosis, and 5 for fibrosis more than 76%. In addition, Masson staining (G1340, Solaibao Life Science Co., Ltd., Beijing, China) was performed. Tissues were then stained in Weigert iron hematoxylin staining solution for 10 min, Masson's blue solution for 5 min, Lichunhong fuchsin staining solution for 10 min and aniline blue staining solution for 2 min. The tissues were rapidly dehydrated using 95% absolute ethanol, cleared in xylene, and sealed by neutral gum. The fibrosis area was assessed through microscopic observation and expressed as %.

Cell culture and treatment

Human renal cortical proximal tubular epithelial cells (HK2; CL-0109, Procell Life Science & Technology Co., Ltd., Wuhan, China) were subcultured in DMEM medium supplemented with 10% fetal bovine serum (Thermo Fisher Scientific, USA) and penicillin streptomycin mixture (Beijing Solaibao Life Science, China) at 37°C and 5% CO₂. The cells at logarithmic phase were further classified into three groups according to different treatment, namely NC group (original medium), TGF-β1 group (10 ng/mL TGF-β1 (P02279, Solaibao Life Science, China)) and TGF-β1 + RR group (10 ng/mL TGF-β1 + 0.23 g/mL RR dissolved in DMEM medium).

Cell transfection and grouping

MiR-122-5p inhibitor and mimic, overexpressed PKM and its negative control (Shanghai Gene Pharmaceutical Co., Ltd., China) were diluted by OptiMEM1 reduced-serum medium (Thermo Fisher Scientific, USA), and the diluted plasmids were transfected into TGF-β1-induced HK2 cells using Lipofectamine 3000 transfection reagent (Thermo Fisher Scientific, USA). The transfection was performed according to the kit instruction. Cells were collected after incubation at 37°C and 5% CO₂ for 48 h. Transfection efficiency was detected by qRT-PCR and western blotting for further experiments. Plasmid sequences are presented in **Table 1**.

The cells were grouped according to different transfections: TGF-β1 + inhibitor NC group (TGF-β1 group cells transfected with negative control of miR-122-5p inhibitor), TGF-β1 + inh-

The effect of RR in renal fibrosis

Table 2. Primer sequence for qRT-PCR

Genes	Sequence (5'-3')
miR-122-5p	F: AATCGGAGCATTGCGCTTATACGAT R: GCTATTACGGAATATCGCGAGCGA
PKM	F: CGCTATAGAAGCGCATTAGCGCA R: TAGCGATCATTACGCGACCCGAGC
FN	F: ATAATCGGCATCTACGGAGCGATCTC R: AGTTCGCGATATCTACGGAGCAGC
Col-I	F: AATCTCGGAGCAGCAGTCTACGC R: CCTATCAGCGAGCGTCTACGCGCGA
GAPDH	F: GCTATGCGCATCGGCTATGCGCAT R: ATACGTGTCAAGAGCTGCGCTAC
U6	F: TAGAGCTCAGGTACGCGTAGCAA R: GCCGAGCGGATCGATTACGGCTA

miR-122-5p group (TGF- β 1 group cells transfected with miR-122-5p inhibitor), TGF- β 1 + RR + inhibitor NC group (TGF- β 1 + RR group cells transfected with negative control of miR-122-5p inhibitor), TGF- β 1 + RR + inh-miR-122-5p group (TGF- β 1 + RR group cells transfected with miR-122-5p inhibitor), TGF- β 1 + pcDNA-NC group (TGF- β 1 group cells transfected with pcDNA-NC vector), TGF- β 1 + pcDNA-PKM group (TGF- β 1 group cells transfected with pcDNA-PKM vector), TGF- β 1 + RR + pcDNA-NC group (TGF- β 1 + RR group cells transfected with pcDNA-NC vector), TGF- β 1 + RR + pcDNA-PKM group (TGF- β 1 + RR group cells transfected with pcDNA-PKM vector), TGF- β 1 + RR + mimic NC group (TGF- β 1 + RR group cells transfected with negative control of miR-122-5p mimic), TGF- β 1 + RR + miR mimic group (TGF- β 1 + RR group cells transfected with miR-122-5p mimic), TGF- β 1 + RR + miR mimic + pcDNA-NC group (TGF- β 1 + RR group cells transfected with miR-122-5p mimic and pcDNA-NC vector), and TGF- β 1 + RR + miR mimic + pcDNA-PKM group (TGF- β 1 + RR group cells transfected with miR-122-5p mimic and pcDNA-PKM vector).

qRT-PCR

The renal tissues were placed in a mortar containing liquid nitrogen and then grounded thoroughly. RNA was extracted from renal tissues and cells respectively using TRIzol reagent (Thermo Fisher Scientific, USA). RNA was reverse-transcribed to synthesize cDNA using PrimeScript RT reagent (Takara Biotechnology Incorporation, Japan) at 37°C for 30 min and then 85°C for 5 s. The levels of target mRNA

were analyzed using SYBR Premix Ex Taq II reagent (Takara Biotechnology Incorporation, Japan) and the 7500 Fast real-time PCR system (American Butter Institute, USA). The reaction condition: 50°C for 2 min, 95°C for 2 min, 95°C for 3 s and 60°C for 30 s, which were repeated 40 times. The total reaction volume was 20 μ L: SYBR Premix Ex Taq (2 \times) 10 μ L, forward primer 0.4 μ L, reverse primer 0.4 μ L, DNA template 2 μ L, and sterilized distilled water 7.2 μ L. 2- $\Delta\Delta$ Ct was used to calculate the results, with U6 as the internal reference for miR-122-5p and GAPDH as the internal reference for the rest. The primers were synthesized by Wuhan Gene Create Biological (China). See **Table 2** for details.

Enzyme-linked immunosorbent assay (ELISA)

Interleukin 6 (IL-6) and tumor necrosis factor- α (TNF- α) levels in mouse serum were measured using ELISA kits (Wuhan Sipei Biotechnology Co., Ltd.). The detection was performed in accordance with the kit instruction.

Western blot

The total proteins from renal tissues were extracted using RIPA lysis buffer (Solaibao Life Science, China). The proteins were incubated on ice for 30 min and centrifuged at 13,000 rpm and 4°C for 10 min. The protein concentrations were analyzed using a BCA protein assay kit (Shanghai Yeasen Biological Technology Co., Ltd., China). A total of 50 μ g of protein samples were separated using 12% sodium dodecyl sulfate polyacrylamide gel electrophoresis and electrotransferred onto the PVDF membrane (Thermo Fisher Scientific, USA). The membrane was placed in 5% skimmed milk for blocking. One hour later, the primary antibodies against fibronectin (FN, 1:1000, ab268020, Abcam, UK), type I collagen (Col-I, 1:1000, ab270993, Abcam, UK), PKM (1:2000, ab150377, Abcam, UK), and GAPDH (1:1000, ab8245, Abcam, UK) were added to the membrane for reaction overnight at 4°C. The secondary antibody horseradish peroxidase-conjugated goat anti-rabbit IgG (1:2000, ab6721, Abcam, UK) was then added and cultured for 1 h at 37°C. Finally, ECL chemiluminescence reagent (Solaibao Life Science, China) was added to the membrane for visualization of protein bands and quantitative analysis was performed using Image J software.

The effect of RR in renal fibrosis

MTT

Cells were seeded in 96-well culture plates at a density of 5×10^4 cells per well and cultured in an incubator for 5 days at 37°C and 5% CO₂. A total of 20 µL of MTT solution (Shanghai Beyotime Biotechnology Co., Ltd., China) was added to each well and cultured for 4 h in an incubator. After discarding the culture medium, 100 µL of DMSO was added, and the solution was placed in the incubator to wait for the dissolve of formazan crystals. The absorbance value at 570 nm was detected using a multi-plate reader (Nanjing Detie Experimental Equipment Co., Ltd., China), and the result was expressed as the value of cell activity of each group/the value of cell activity of the control group $\times 100\%$.

Flow cytometry

The Annexin V-FITC/PI Apoptosis Detection Kit (TransGen Biotechnology Co., Ltd., China) was applied. Cells were suspended in PBS, collected by centrifugation, washed with precooled PBS, centrifuged at 500× g and 4°C for 5 min. Then the cells were collected, resuspended in 100 µL of 1× Annexin V binding buffer, mixed fully with 5 µL of Annexin V-FITV and 5 µL of PI staining solution, and incubated in a dark room for 15 min. Apoptosis was reflected by a Flow cytometer (Beckman Coulter, USA).

Dual-luciferase reporter assay

A dual-luciferase reporter assay was designed to validate the targeting relationship between miR-122-5p and PKM based on the binding site of miR-122-5p shown in the StarBase website. The 3' UTR end fragment of PKM containing the miR-122-5p binding site was amplified, and site-directed mutation was carried out in the region of PKM 3' UTR using the Quick Mutation™ Gene Site-Directed Mutagenesis Kit (Beyotime Biotechnology Co., Ltd., China), and the wild-type and mutant fragments were cloned into a luciferase reporter vector, named PKM-WT and PKM-MUT. Cells were seeded in 96-well plates at 1×10^4 cells per well and cultured for 24 h for transfection. PKM-WT and PKM-MUT were co-transfected into cells with mimic NC and miR-122-5p mimic, respectively, using Lipofectamine 3000 transfection reagent (Thermo Fisher Scientific, USA) and they were

cultured for 48 hours. Luciferase activity was assessed by the Dual-Luciferase Reporter Assay Kit (Beyotime Biotechnology Co., Ltd., China).

Statistical analysis

In this study, SPSS 23.0 software was used for statistical analysis. Student's t test was included for comparison of differences between two groups. One-way analysis of variance method with Tukey test was utilized for comparison of differences among multiple groups. Correlation analysis between miR-122-5p and PKM was assessed using Spearman correlation analysis. Values are expressed in mean \pm standard deviation. $P < 0.05$ was considered statistically significant.

Results

RR could improve renal function and inhibit renal pathological changes in mice

HE and Masson staining were carried out to observe the pathological damage of renal tissues. HE staining showed that UUO could lead to tubular edema, glomerular basement membrane thickening, and tubular cell disarrangement in mice (**Figure 1A-C**). The results of Masson staining showed that the renal interstitial collagen fiber deposition was obviously observed in renal tissues of UUO mice, but RR could significantly reduce the deposition of collagen fibers (**Figure 1B-D**). Cr and BUN are common indicators for renal function, and up-regulation of these indicators indicates abnormal renal function. The results of this study showed that UUO could induce the up-regulation of Cr and BUN in mice, while RR could further inhibit the up-regulation of Cr and BUN induced by UUO (**Figure 1E, 1F**, all $P < 0.05$). The above experiments demonstrated that RR had a protective effect on the kidneys of UUO mice.

RR had the effects of anti-inflammation and anti-renal fibrosis

We investigated the anti-inflammation and anti-renal fibrosis effects of RR in UUO mice. An increase in IL-6 and TNF- α levels in the serum of UUO mice was observed, while these levels were decreased under RR intervention (**Figure 2A**, all $P < 0.05$). Similarly, UUO induced

The effect of RR in renal fibrosis

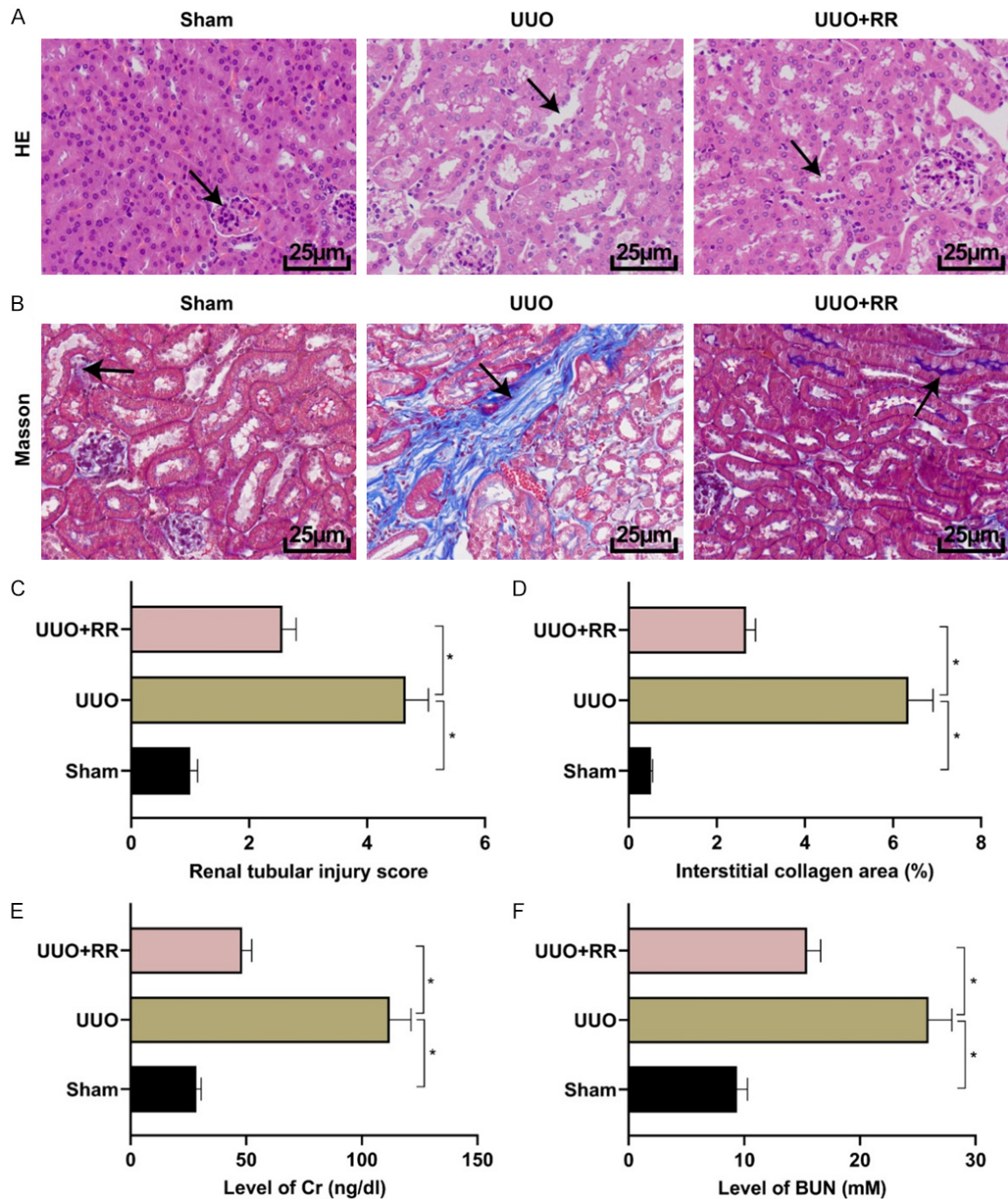


Figure 1. RR could improve renal function and inhibit renal pathological changes in mice. A. HE staining (The arrows indicated injured cells and tubular basement membrane) (400×). B. Masson staining (The blue part indicated by the arrow indicated tissue collagen fiber deposition; 400×). C. HE staining quantitative results. D. Masson staining quantitative results. E. Cr level detection. F. BUN level detection. n=10, *P<0.05.

increased mRNA of FN and Col-I and protein levels in the mouse kidney, while RR intervention led to decreased mRNA protein levels of FN and Col-I (Figure 2B-D, all P<0.05), indicating that RR could alleviate UUO-induced inflammatory injury and renal fibrosis.

RR regulated miR-122-5p expression

The analysis of the GSE162794 profile in the GEO database revealed that miR-122-5p was significantly up-regulated in the Sham group and largely down-regulated in the UUO group

The effect of RR in renal fibrosis

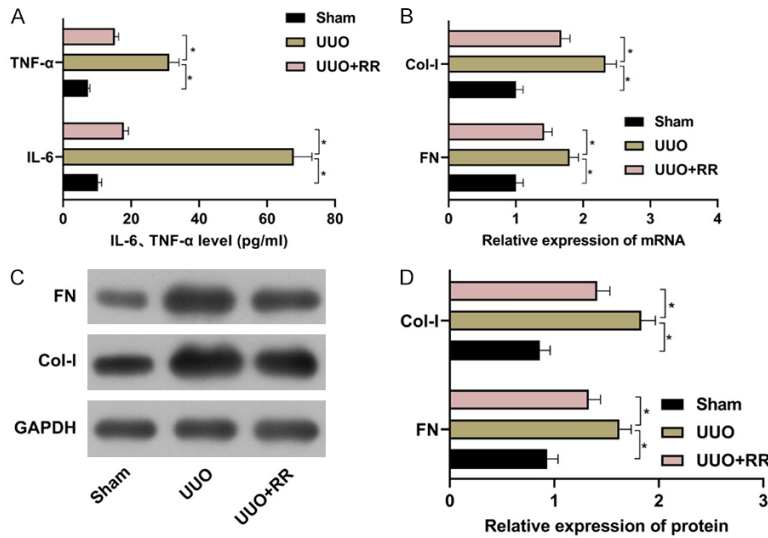


Figure 2. RR had the anti-inflammatory and anti-renal fibrosis effects. A. Detection of IL-6 and TNF- α levels. B. Detection of mRNA levels of FN and Col-I. C, D. Detection of protein levels of FN and Col-I. n=10, *P<0.05.

(Figure 3A-C). In order to prove it, we detected the expression levels of miR-122-5p in the renal tissues of mice in each group using qRT-PCR, and the results showed that miR-122-5p expression was decreased in mice of the UUO group compared with that of the sham group; it was increased in mice of the UUO + RR group compared with that of the UUO group (Figure 3D, P<0.05). The same result was obtained in the *in vitro* cell model that miR-122-5p expression was decreased in cells of the TGF- β 1 group compared with that of the NC group, but it was increased in cells of the TGF- β 1 + RR group compared with that of the TGF- β 1 group (Figure 3E, P<0.05). The above experiments indicated that RR could regulate miR-122-5p.

Down-regulation of miR-122-5p could promote the progression of in vitro models and eliminate the protective effect of RR

We further explored the role of miR-122-5p in renal fibrosis. First, inh-miR-122-5p was transfected into cells of TGF- β 1 group, and the results displayed that the expression of miR-122-5p in cells of TGF- β 1 group was significantly inhibited compared with that in cells of inhibitor NC group (Figure 4A, P<0.05). In functional experiments, it was found that transfection of inh-miR-122-5p into cells of TGF- β 1 group could significantly increase the levels of

IL-6, TNF- α , FN, and Col-I, inhibit the cell viability, and induce apoptosis (all P<0.05). Cells treated with RR led to completely opposite results (all P<0.05). When inh-miR-122-5p was transfected into RR-treated cells, the inhibitory effects of RR on IL-6, TNF- α , FN, and Col-I were partially reversed, cell viability was reduced, and apoptosis was increased (all P<0.05), as shown in Figure 4B-G. These experimental data demonstrated that down-regulation of miR-122-5p could aggravate the progression of injury in *in vitro* model, and attenuate the protective effect of RR on cells.

A targeting relationship was proved between miR-122-5p and PKM

The downstream target genes of miR-122-5p were predicted using TargetScan and StarBase online tools, and the results were intersected (Figure 5A) to perform pathway annotation analysis of the intersected genes (Figure 5B). Glycolysis/gluconeogenesis pathway was found and renal injury was associated with the accumulation of intermediate product of glycolysis. DisGENET website was included to search for renal fibrosis risk genes. The genes (G6PC3, PKM, G6PC, DLAT, ALDOA) enriched in the pathway were analyzed for protein interaction with renal fibrosis risk genes. It was found that PKM was more closely linked to other genes in the analysis results (Figure 5C). A dual-luciferase reporter assay was designed to validate the targeting relationship between miR-122-5p and PKM. It turned out that miR-122-5p mimic could significantly inhibit the luciferase activity of PKM-WT and the targeting relationship was confirmed (Figure 5D, P<0.05).

PKM expression was upregulated in both UUO mouse tissues and TGF- β 1-treated cells (Figure 6A, 6B, all P<0.05). In addition, miR-122-5p showed a negative correlation with the expression of PKM (Figure 6C, P<0.05), and the expression of PKM in miR-122-5p mimic group was inhibited compared with that in mimic NC

The effect of RR in renal fibrosis

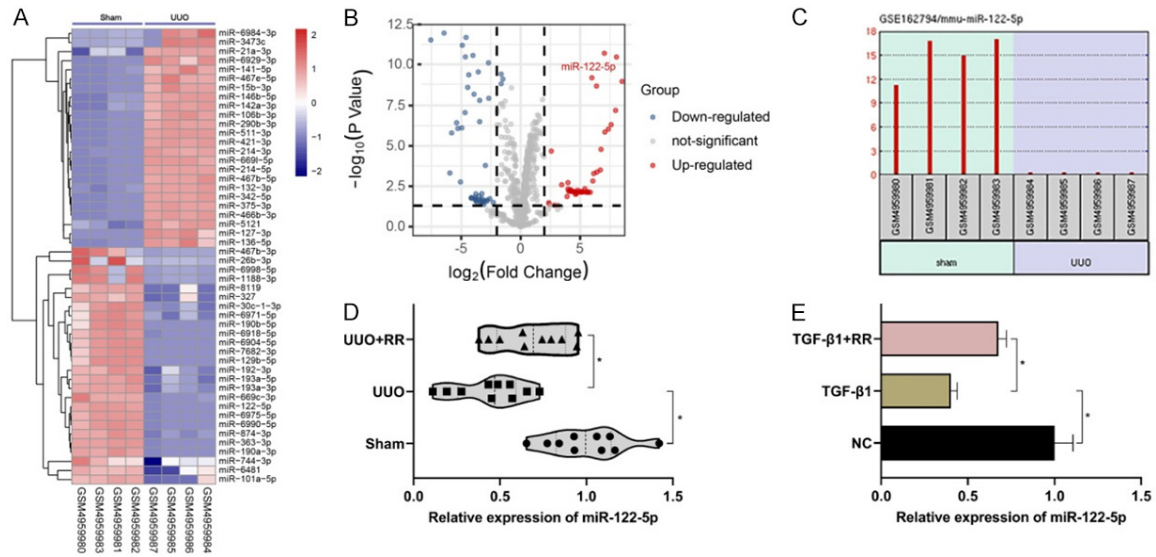


Figure 3. RR could regulate miR-122-5p with PKM. A. Heatmap of differentially expressed miRNAs in the dataset of GSE162794 (Sham:UUO). B. Volcano map of up- and down-regulated miRNAs (Sham:UUO). C. Expression level of miR-122-5p in GSE162794 dataset samples. D, E. Detection of expression levels of miR-122-5p in mouse renal tissue versus HK2 cells. n=10, *P<0.05.

group (Figure 6D, all P<0.05). RR could also interfere with PKM expression (Figure 6A, 6B, all P<0.05). Besides, we found a relationship between PKM and related genes of RR components (Figure 6E). These results suggested that there was a targeting relationship between miR-122-5p and PKM, and RR could regulate the expression of PKM.

Up-regulation of PKM could promote the progress of in vitro models and eliminate the protective effect of APG

To investigate whether PKM was involved in the mechanism of RR protection, we explored the role of PKM in renal fibrosis and its effect on RR. Functional experiments showed that overexpression of PKM in TGF-β1-induced cells significantly increased the levels of IL-6, TNF-α, FN, and Col-I, inhibited cell viability, and increased apoptosis (all P<0.05), which were contrast to the results produced by RR. After further transfection of PKM in RR treatment group, the levels of IL-6, TNF-α, FN, and Col-I, which were inhibited at first, were increased, cell viability was decreased, and apoptosis was induced (all P<0.05), as shown in Figure 7A-F. The above experiments indicated that overexpression of PKM could promote injury in *in vitro* model and inhibit the protective effect of RR on cells.

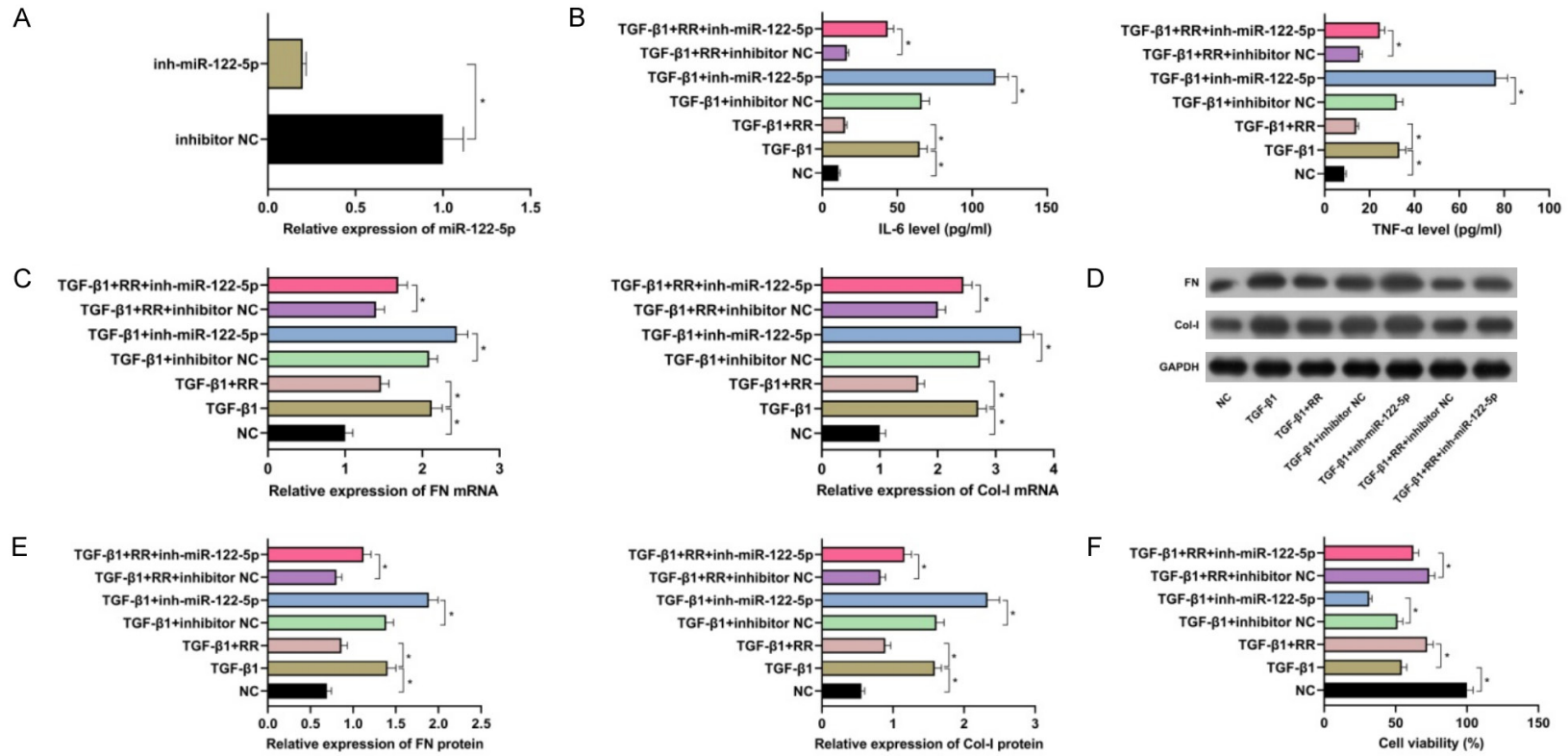
Overexpression of miR-122-5p could inhibit the progression of renal fibrosis in vitro, which was partially counteracted by PKM

To investigate the combined effect of miR-122-5p and PKM, functional rescue experiments were performed. The results revealed that overexpression of miR-122-5p in TGF-β1 and RR-treated cells could further improve the inhibitory effect of RR on the expression levels of IL-6, TNF-α, FN, and Col-I. Meanwhile, the cell viability was significantly increased and the apoptosis rate was largely reduced. However, after transfection with PKM, the promoting effect of miR-122-5p overexpression was weakened, the expression levels of IL-6, TNF-α, FN, and Col-I were up-regulated, the cell viability was reduced, and the apoptosis rate was increased (see Figure 8). It showed that overexpression of miR-122-5p could promote the protective effect of RR on the *in vitro* injury model, but PKM could partially reverse this effect, indicating that miR-122-5p promoted the protective effect of RR on the progression of renal fibrosis by inhibiting PKM.

Discussion

Renal fibrosis is the final pathological result in all kidney diseases [19]. The kidney is stimulated by various pathogenic factors such as trau-

The effect of RR in renal fibrosis



The effect of RR in renal fibrosis

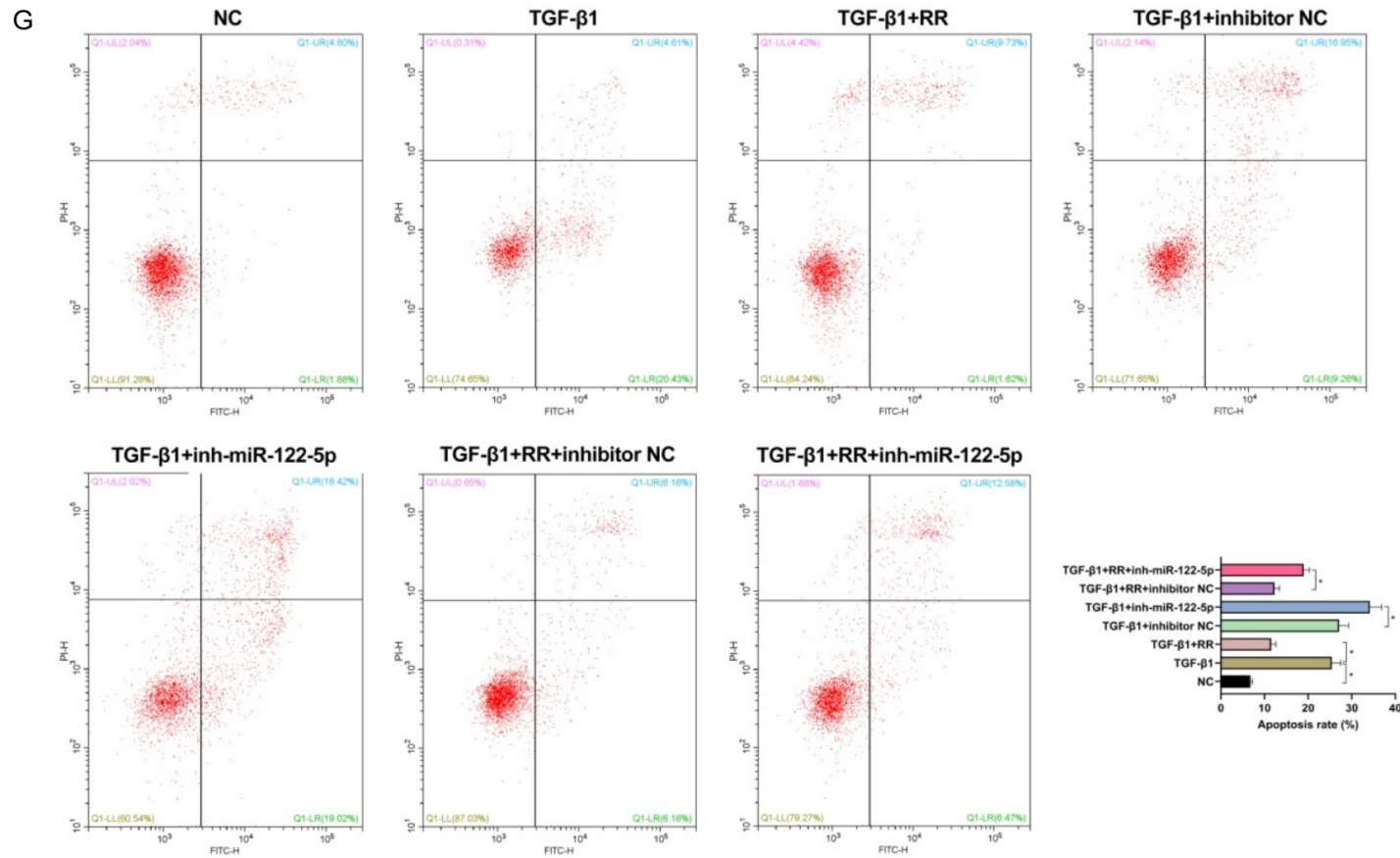


Figure 4. Down-regulation of miR-122-5p could promote the progression of injury in *in vitro* models and eliminate the protective effect of RR *in vitro*. A. Detection of transfection efficiency of inh-miR-122-5p (n=3). B. Detection of IL-6 and TNF- α levels (n=3). C. Detection of mRNA levels of FN and Col-I (n=3). D, E. Detection of protein levels of FN and Col-I (n=3). F. MTT assay of cell viability (n=3). G. Flow cytometry assay of apoptosis (n=3). *P<0.05.

The effect of RR in renal fibrosis

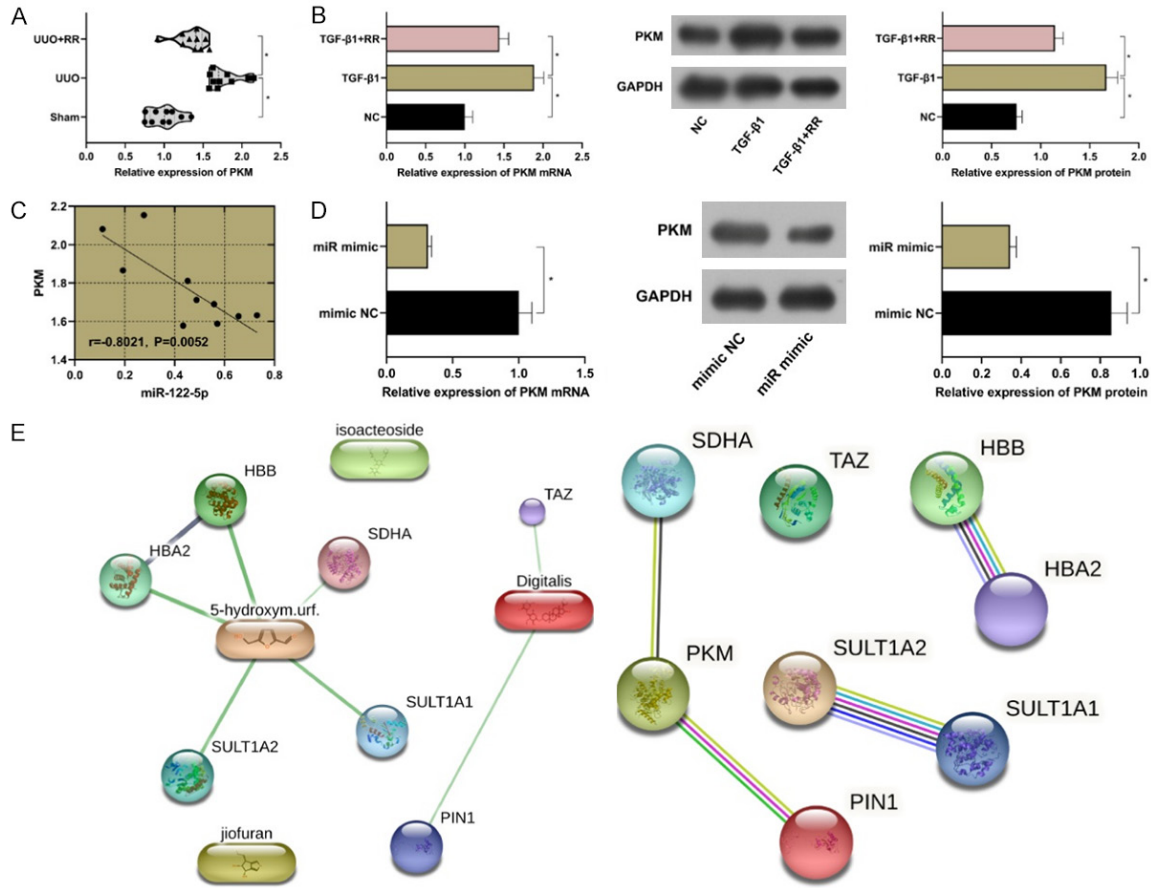


Figure 6. Evaluation of PKM expression. A, B. Detection of PKM expression levels in mouse renal tissues (n=10) and HK2 cells (n=3). C. Correlation analysis results between miR-122-5p and PKM (n=3). D. Effect of miR-122-5p mimic on PKM expression. E. A target relationship was proved between PKM and RR (genes related to RR components on the left and protein interaction analysis between PKM and genes related to RR components on the right). *P<0.05.

In our study, we found that the therapeutic mechanism of RR may be associated with the abnormal expressions of miR-122-5p and PKM. A previous study suggested that miR-122-5p expression was significantly reduced in aristolochic acid-induced renal injury and tubulointerstitial fibrosis [16]. MiR-122-5p expression was decreased in both serum and tubular epithelial cells treated by uric acid from patients with uric acid nephropathy, and the low expression of miR-122-5p might be associated with renal injury in patients [25]. MiR-122-5p expression was decreased in drug-induced renal tubular and glomerular injury models [26]. In this study, miR-122-5p expression was found decreased in UUO mouse tissues and *in vitro* cell models, and RR could increase the expression of miR-122-5p. *In vitro* functional experiments showed that inhibition of miR-122-5p

could promote cell fibrosis and inflammatory injury, reduce cell viability and increase the apoptotic rate, in contrast to the effect of RR. We also found an association between PKM and related genes of RR active ingredients through the bioinformatics tools. In addition, PTBP1 has been shown to play a tumorigenic role in renal cancer by regulating alternative splicing of PKM2 [27]. SGLT2 inhibitors have also been found to reduce hypoxia-induced PKM expression in human renal tubular epithelial cells, which in turn alleviates the injury caused by diabetic nephropathy [28]. In this study, PKM expression was found increased in UUO mouse tissues and *in vitro* cell models, and RR could inhibit the expression of PKM. *In vitro* functional experiments showed that PKM could promote cell fibrosis and inflammatory injury, reduce cell viability and increase the

The effect of RR in renal fibrosis

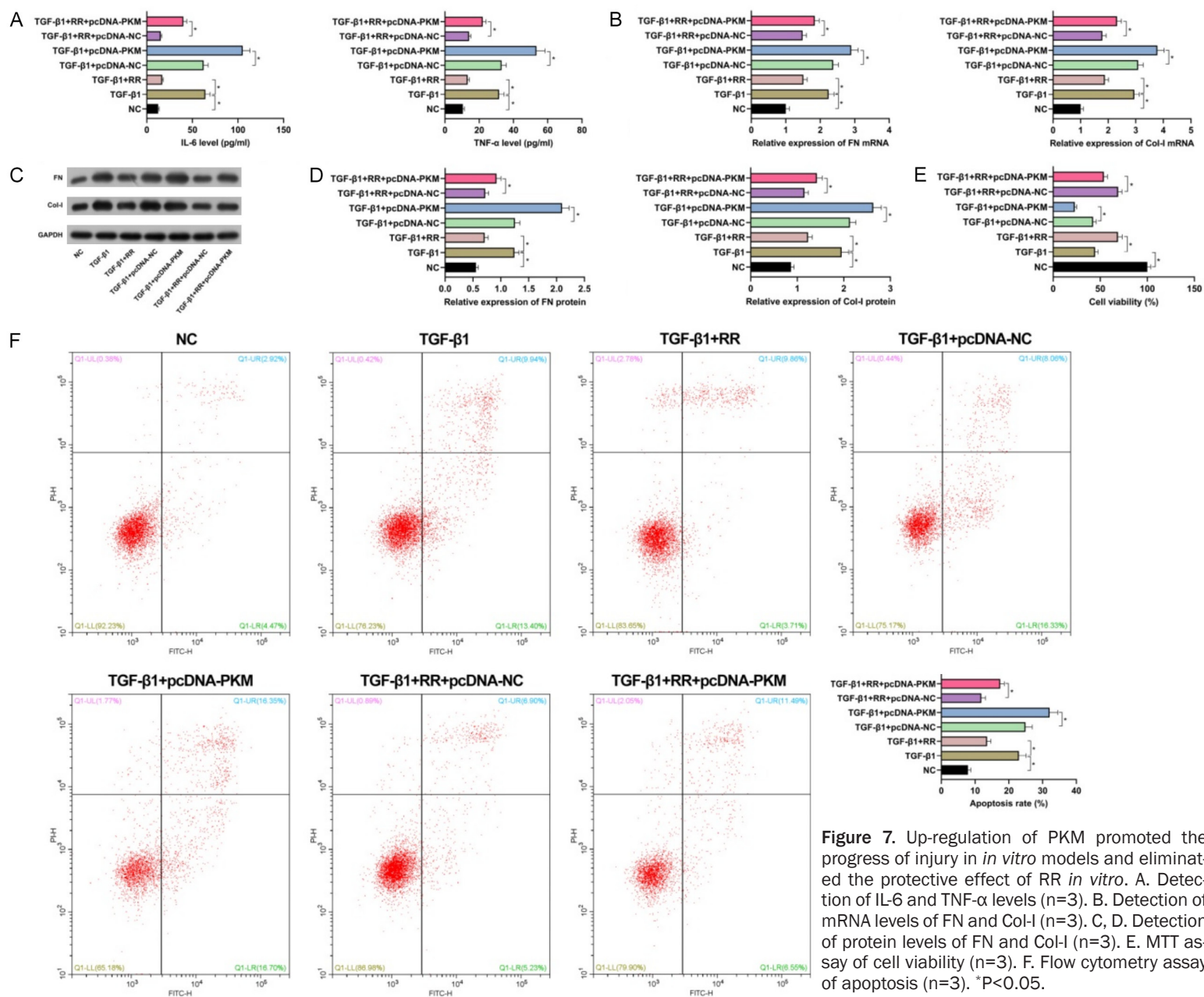


Figure 7. Up-regulation of PKM promoted the progress of injury in *in vitro* models and eliminated the protective effect of RR *in vitro*. **A.** Detection of IL-6 and TNF- α levels (n=3). **B.** Detection of mRNA levels of FN and Col-1 (n=3). **C, D.** Detection of protein levels of FN and Col-1 (n=3). **E.** MTT assay of cell viability (n=3). **F.** Flow cytometry assay of apoptosis (n=3). *P<0.05.

The effect of RR in renal fibrosis

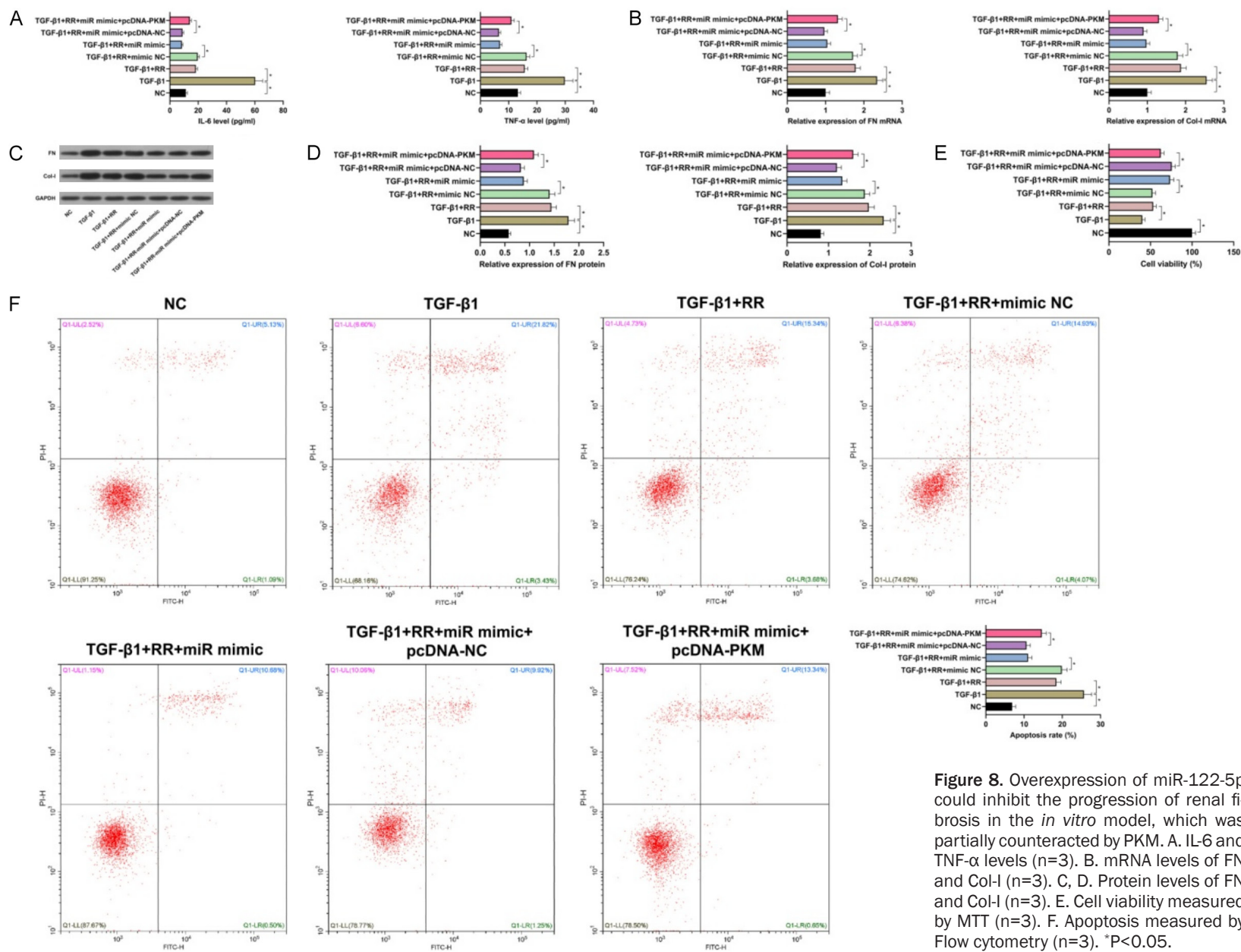


Figure 8. Overexpression of miR-122-5p could inhibit the progression of renal fibrosis in the *in vitro* model, which was partially counteracted by PKM. A. IL-6 and TNF- α levels (n=3). B. mRNA levels of FN and Col-I (n=3). C, D. Protein levels of FN and Col-I (n=3). E. Cell viability measured by MTT (n=3). F. Apoptosis measured by Flow cytometry (n=3). *P<0.05.

The effect of RR in renal fibrosis

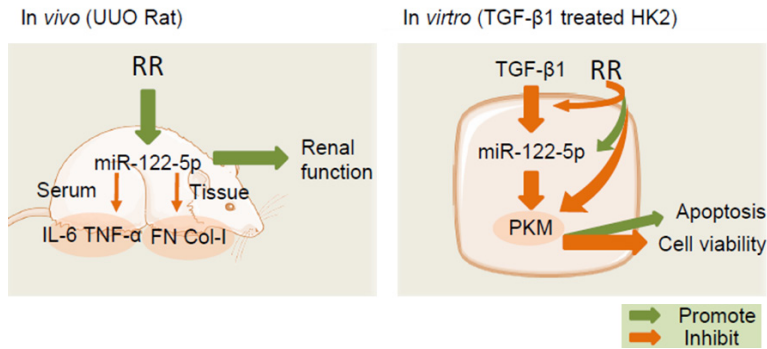


Figure 9. The mechanism by which Rehmannia Glutinosa regulates miR-122-5p/PKM axis to inhibit the progression of renal fibrosis.

apoptotic rate, in contrast to the effect of RR. Taken together, it is suggested that the effect of RR may be correlated with the expressions of miR-122-5p and PKM.

In addition, we also confirmed the targeted regulatory relationship between miR-122-5p and PKM, and overexpression of miR-122-5p could inhibit the expression of PKM, which has also been confirmed in a previous study [29]. The combined effect of RR with miR-122-5p and PKM was also confirmed in this study, i.e., the overexpression of miR-122-5p could promote the protective effect of RR but this effect was partially counteracted by PKM. The role of miR-122-5p with PKM in renal fibrosis was further demonstrated in this study. In addition, the inhibition of miR-122-5p or up-regulation of PKM could significantly attenuate the anti-fibrotic effect of RR, which showed that RR might play an anti-fibrotic role in cells by regulating the miR-122-5p/PKM axis.

The innovation of this study is the further demonstration of the molecular mechanism of RR in anti-fibrosis by regulating the miR-122-5p/PKM axis. However, there are still many shortcomings in this study. For example, the exploration of miR-122-5p downstream target genes was not in-depth, and the signaling pathways in the RR-regulated molecular network were not explored.

In summary, this is the first study to propose RR as a new target for the treatment of renal fibrosis by promoting miR-122-5p and inhibiting PKM to improve the pathological damage of renal fibrosis. The mechanism of this study is illustrated in **Figure 9**.

Acknowledgements

This work was supported by the Shandong TCM Science and Technology Development Project, Qingdao Medical and Health Excellent Talents Training Program (2017-333).

Disclosure of conflict of interest

None.

Address correspondence to:

Xiangbo Sun, Department of Nephrology, Hiser Medical Center of Qingdao, No. 4 Renmin Road, Qingdao 266000, Shandong Province, China. Tel: +86-18661831982; E-mail: sunxiangbo8f9f@163.com

References

- [1] Berg P, Jeppesen M and Leipziger J. Cystic fibrosis in the kidney: new lessons from impaired renal HCO₃-excretion. *Curr Opin Nephrol Hypertens* 2021; 30: 437-443.
- [2] Mylonas KJ, O'Sullivan ED, Humphries D, Baird DP, Docherty MH, Neely SA, Krimpenfort PJ, Melk A, Schmitt R, Ferreira-Gonzalez S, Forbes SJ, Hughes J and Ferenbach DA. Cellular senescence inhibits renal regeneration after injury in mice, with senolytic treatment promoting repair. *Sci Transl Med* 2021; 13: eabb0203.
- [3] Gao Y, Yuan D, Gai L, Wu X, Shi Y, He Y, Liu C, Zhang C, Zhou G and Yuan C. Saponins from panax japonicus ameliorate age-related renal fibrosis by inhibition of inflammation mediated by NF-κB and TGF-β1/Smad signaling and suppression of oxidative stress via activation of Nrf2-ARE signaling. *J Ginseng Res* 2021; 45: 408-419.
- [4] Doke T, Huang S, Qiu C, Liu H, Guan Y, Hu H, Ma Z, Wu J, Miao Z, Sheng X, Zhou J, Cao A, Li J, Kaufman L, Hung A, Brown CD, Pestell R and Susztak K. Transcriptome-wide association analysis identifies DACH1 as a kidney disease risk gene that contributes to fibrosis. *J Clin Invest* 2021; 131: e141801.
- [5] Wang X, Wu C, Xu M, Cheng C, Liu Y and Di X. Optimisation for simultaneous determination of iridoid glycosides and oligosaccharides in radix rehmannia by microwave assisted extraction and HILIC-UHPLC-TQ-MS/MS. *Phytochem Anal* 2020; 31: 340-348.
- [6] Gao Z, Lu Y, Halmurat U, Jing J and Xu D. Study of osteoporosis treatment principles used historically by ancient physicians in Chinese medicine. *Chin J Integr Med* 2013; 19: 862-868.

The effect of RR in renal fibrosis

- [7] Xia T, Dong X, Jiang Y, Lin L, Dong Z, Shen Y, Xin H, Zhang Q and Qin L. Metabolomics profiling reveals rehmanniae radix preparata extract protects against glucocorticoid-induced osteoporosis mainly via intervening steroid hormone biosynthesis. *Molecules* 2019; 24: 253.
- [8] Soliman AM, Teoh SL, Ghafar NA and Das S. Molecular concept of diabetic wound healing: effective role of herbal remedies. *Mini Rev Med Chem* 2019; 19: 381-394.
- [9] Zhang X, Wang D, Ren X, Atanasov AG, Zeng R and Huang L. System bioinformatic approach through molecular docking, network pharmacology and microarray data analysis to determine the molecular mechanism underlying the effects of rehmanniae radix praeparata on cardiovascular diseases. *Curr Protein Pept Sci* 2019; 20: 964-975.
- [10] Xu R, Luo C, Ge Q, Ying J, Zhang P, Xia C, Fang L, Xu H, Yuan W, Xu T, Lv S, Jin H, Tong P, Tian K and Wang P. Radix rehmanniae praeparata promotes bone fracture healing through activation of TGF- β signaling in mesenchymal progenitors. *Biomed Pharmacother* 2020; 130: 110581.
- [11] Chen J, Chen Y, Shu A, Lu J, Du Q, Yang Y, Lv Z and Xu H. Radix rehmanniae and corni fructus against diabetic nephropathy via AGE-RAGE signaling pathway. *J Diabetes Res* 2020; 2020: 8358102.
- [12] Liu F, Deng W, Wan Z, Xu D, Chen J, Yang X and Xu J. lncRNA MAGI2-AS3 overexpression had antitumor effect on hepatic cancer via miRNA-23a-3p/PTEN axis. *Food Sci Nutr* 2021; 9: 2517-2530.
- [13] Sun CM, Zhang WY, Wang SY, Qian G, Pei DL and Zhang GM. microRNA let-7i-5p aggravates kidney fibrosis via targeting GALNT1. *Gen Physiol Biophys* 2021; 40: 147-154.
- [14] Zhou J, Zhou H, Liu Y and Liu C. Inhibition of CTCF-regulated miRNA-185-5p mitigates renal interstitial fibrosis of chronic kidney disease. *Epigenomics* 2021; 13: 859-873.
- [15] Yi L, Ai K, Li H, Qiu S, Li Y, Wang Y, Li X, Zheng P, Chen J, Wu D, Xiang X, Chai X, Yuan Y and Zhang D. CircRNA_30032 promotes renal fibrosis in UUO model mice via miRNA-96-5p/HBEGF/KRAS axis. *Aging (Albany NY)* 2021; 13: 12780-12799.
- [16] Zhu Z, Xu X, Wang F, Song Y, Zhu Y, Quan W, Zhang X, Bi C, He H, Li S and Li X. Integrative microRNA and mRNA expression profiling in acute aristolochic acid nephropathy in mice. *Mol Med Rep* 2020; 22: 3367-3377.
- [17] Yin XN, Wang J, Cui LF and Fan WX. Enhanced glycolysis in the process of renal fibrosis aggravated the development of chronic kidney disease. *Eur Rev Med Pharmacol Sci* 2018; 22: 4243-4251.
- [18] Cao D, Wang Y, Zhang Y, Zhang Y, Huang Q, Yin Z, Cai G, Chen X and Sun X. Regulation of connective tissue growth factor expression by miR-133b for the treatment of renal interstitial fibrosis in aged mice with unilateral ureteral obstruction. *Stem Cell Res Ther* 2021; 12: 171.
- [19] Liu TT, Luo R, Yang Y, Cheng YC, Chang D, Dai W, Li YQ, Ge SW and Xu G. LRG1 mitigates renal interstitial fibrosis through alleviating capillary rarefaction and inhibiting inflammatory and pro-fibrotic cytokines. *Am J Nephrol* 2021; 52: 228-238.
- [20] Wang Q, Tao Y, Xie H, Liu C and Liu P. MicroRNA-101 Inhibits renal tubular epithelial-to-mesenchymal transition by targeting TGF- β 1 type I receptor. *Int J Mol Med* 2021; 47: 119.
- [21] Zhang Y, Zhang R and Han X. Disulfiram inhibits inflammation and fibrosis in a rat unilateral ureteral obstruction model by inhibiting gasdermin D cleavage and pyroptosis. *Inflamm Res* 2021; 70: 543-552.
- [22] Zhang H, Wu ZM, Yang YP, Shaikat A, Yang J, Guo YF, Zhang T, Zhu XY, Qiu JX, Deng GZ and Shi DM. Catalpol ameliorates LPS-induced endometritis by inhibiting inflammation and TLR4/NF- κ B signaling. *J Zhejiang Univ Sci B* 2019; 20: 816-827.
- [23] Gong W, Zhang N, Cheng G, Zhang Q, He Y, Shen Y, Zhang Q, Zhu B, Zhang Q and Qin L. Rehmannia glutinosa libosch extracts prevent bone loss and architectural deterioration and enhance osteoblastic bone formation by regulating the IGF-1/PI3K/mTOR pathway in streptozotocin-induced diabetic rats. *Int J Mol Sci* 2019; 20: 3964.
- [24] Chao CH, Hsu JL, Chen MF, Shih YH, Lee CH, Wu ML and Chang CI. Anti-hypertensive effects of radix rehmanniae and its active Ingredients. *Nat Prod Res* 2020; 34: 1547-1552.
- [25] Hu JC, Wu H, Wang DC, Yang ZJ and Dong JJ. LncRNA ANRIL promotes NLRP3 inflammatory activation in uric acid nephropathy through miR-122-5p/BRCC3 axis. *Biochimie* 2019; 157: 102-110.
- [26] Kagawa T, Zárýbnický T, Omi T, Shirai Y, Toyokuni S, Oda S and Yokoi T. A scrutiny of circulating microRNA biomarkers for drug-induced tubular and glomerular injury in rats. *Toxicology* 2019; 415: 26-36.
- [27] Jiang J, Chen X, Liu H, Shao J, Xie R, Gu P and Duan C. Polypyrimidine tract-binding protein 1 promotes proliferation, migration and invasion in clear-cell renal cell carcinoma by regulating alternative splicing of PKM. *Am J Cancer Res* 2017; 7: 245-259.

The effect of RR in renal fibrosis

- [28] Ryoichi B, Yumi T, Takao T, Hiroya, Yasutaka T, Hidemitsu S and Tsuguhito O. Hypoxia-inducible factor-1 α is the therapeutic target of the SGLT2 inhibitor for diabetic nephropathy. *Sci Rep* 2019; 9: 14754.
- [29] Wang S, Zheng W, Ji AL, Zhang DH and Zhou M. Overexpressed miR-122-5p promotes cell viability, proliferation, migration and glycolysis of renal cancer by negatively regulating PKM2. *Cancer Manag Res* 2019; 11: 9701-9713.